Nanoconjugates

DOI: 10.1002/anie.201106313

ImmunoPods: Polymer Shells with Native Antibody Cross-Links**

*Ke Zhang, Dan Zheng, Liangliang Hao, Joshua I. Cutler, Evelyn Auyeung, and Chad A. Mirkin**

Recently, we described the discovery of a novel gold nanoparticle (AuNP) catalyzed reaction, which allows one to make heavily cross-linked polymer shells on the surface of the NP.[1] With this reaction, the NP acts both as a scaffold and catalyst to facilitate the cross-linking of linear polymers with propargyl ether side chains. Specifically, it has been postulated that hydroxy groups, formed from the hydrolysis of the propargyl ethers, add to the alkynes adsorbed on the gold surface, leading to cross-linking of the polymer.[2] Importantly, the NP core can be subsequently removed to form hollow polymer nanopods. These structures, which are highly adaptable through choice of polymer and AuNP template, show promise for many applications, spanning molecular diagnostics,[3] drug delivery,[4] materials synthesis, and colloidal crystal design.[5] However, before they can be fully utilized, methods for functionalizing them with bioactive structures must be developed. In this regard, we have devised methods for making nanopods from oligonucleotides with modified bases to generate polyvalent oligonucleotide nanostructures, which now constitute an entire class of single-entity intracellular gene regulation agents.[6] Herein, we address the challenge of creating nanopods functionalized with antibodies (Abs) by creating a class of materials, termed immunopods (IPs), structures that can be made from Abs and the appropriate linear polymers with propragyl ether side chains in a one-pot fashion, and then explore their ability to selectively target cells. IPs are important entries in the class of structures that can be made by gold-particle surface-templated and catalyzed approaches since they can enable a wide variety of pharmaceutical studies and potential applications.

Given the broad utility of Ab–NP conjugates, many strategies to attach an Ab to surfaces have been developed. These strategies largely fall into two categories: specific and nonspecific.[7] In nonspecific attachment methods, van der Waals or electrostatic interactions are typically utilized. However, successful in vivo application often requires structures that do not nonspecifically bind to cells, making surfaces composed of nonsticking materials such as polyethylene glycol (PEG) or poly-*N*-vinylpyrrolidone (PVP) highly desirable. Therefore, nonspecific adhesion of antibodies to these materials is often ineffective. To functionalize NPs by using specific interactions, both covalent and noncovalent forces have been exploited. For example, biotinylated Abs have been routinely used to modify streptavidin (SA) coated surfaces.[8] Caruso and co-workers have recently shown by using click chemistry that monoclonal Abs can be conjugated through a PEG tether to nonfouling PVP nanocapsules.[9] Meier and co-workers demonstrated efficient and selective functionalization of 4-formylbenzoate-functionalized polymersomes with antibodies containing 6-hydrazinonicotinate acetone hydrazine moieties.[10] Other common approaches include carbodiimide coupling, aldehyde/amine coupling, and thiol/maleimide coupling.[7b] However, many useful conjugation strategies require Ab modification, before surface functionalization, which not only increases the complexity, but also the cost of preparation. Herein, we show how IPs can be rapidly made by using the aforementioned catalytic-templating approach by sequentially coadsorbing the antibody and polymer during the nanopod synthesis. We postulated that amine-rich antibodies could act as the nucleophiles that are essential in the cross-linking step (normally hydroxy groups), thereby incorporating native Abs into the polymer shell in a one-pot fashion (Figure 1).

To test this hypothesis, we designed a two-protein-based model system that one can use to evaluate the successful incorporation of the proteins in a bioactive form within the polymer shell. The model system uses SA as a surface-anchoring moiety and horseradish peroxidase (HRP) as a reporter moiety (Figure 2 A). If the two proteins are success-

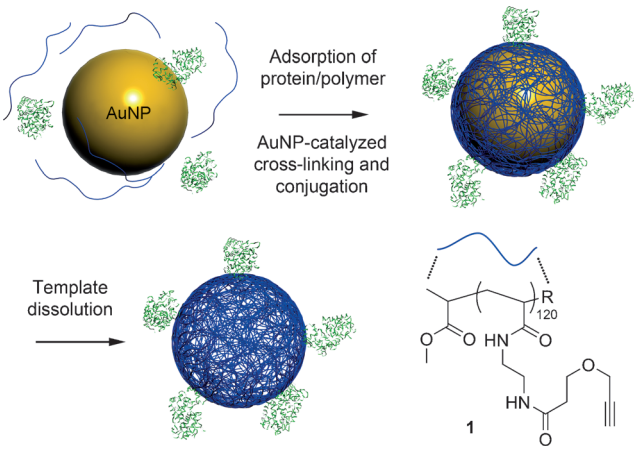

Figure 1. Synthesis of protein-conjugated hollow polymer nanopods (R = Br or -$NHCH_2CH_2NHCOCH_2CH_2OCH_2CCH$).

[*] Dr. K. Zhang, D. Zheng, L. Hao, J. I. Cutler, E. Auyeung, Prof. C. A. Mirkin
Department of Chemistry, Northwestern University
2145 Sheridan Road, Evanston, IL 60208-3113 (USA)
E-mail: chadnano@northwestern.edu

[**] C.A.M. acknowledges the NCI-CCNE, NSF, and AFOSR/MURI for support of this research. E.A. acknowledges the NDSEG for a Graduate Research Fellowship. The transmission electron microscopy was carried out in the EPIC facility at the NUANCE Center at Northwestern University. The NUANCE Center is supported by NSF-NSEC, NSF-MRSEC, the Keck Foundation, the State of Illinois, and Northwestern University. Infrared spectroscopy and mass spectrometry was conducted at the IMSERC facility at Northwestern University.

Supporting information for this article is available on the WWW under http://dx.doi.org/10.1002/anie.201106313.

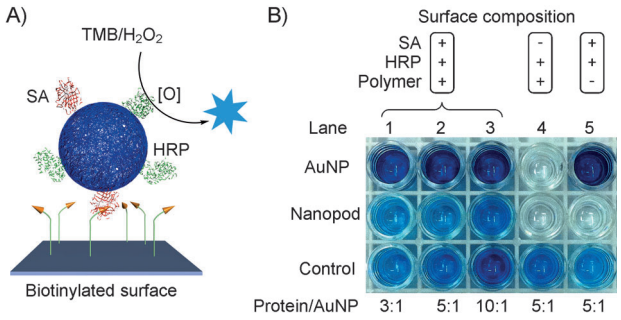

Figure 2. A) A two-protein reporter assay designed to evaluate the successful formation of protein-nanopod conjugates. B) The blue color indicates that HRP-modified particles are immobilized on the biotinylated surface after extensive washing (except bottom row). Lanes 1–3: samples containing SA, HRP, and polymer **1**; lanes 4 and 5: control samples lacking either SA or polymer **1**. Top row: AuNP–protein conjugates; middle row: protein–nanopod conjugates; bottom row: protein–nanopod conjugates directly combined with 3,3′,5,5′-tetramethylbenzidine (TMB)/H_2O_2 developing solution as a control to determine if HRP remains active after dissolution of the gold core. This assay indicates that protein–nanopod conjugates containing both HRP and SA are successfully formed.

fully incorporated into the nanopods, incubation on a biotin-coated surface would lead to their immobilization, and the HRP can then catalyze the oxidation of tetramethylbenzidine (TMB) by H_2O_2, producing an intense blue color which can be visually examined. Failure of either protein to be incorporated into the nanopod shell or the loss of protein function would result in a negative (colorless) readout.

The synthesis begins by allowing the proteins to adsorb onto 10 nm AuNPs, prepared by literature methods.[11] Dynamic light scattering (DLS) studies confirmed the adsorption by showing an increase in the particle size from (10.2 ± 1.8) nm (citrate-stabilized AuNP) to (18.6 ± 3.1) nm, as expected from the respective sizes of the AuNP, SA (52.8 kDa, ca. 4 nm), and HRP (44.2 kDa, ca. 4 nm). Addition of polymer **1** to the protein–gold conjugates does not result in a significant change in the size ((18.9 ± 4.1) nm) which suggests that the proteins remain on the surface of the AuNP, as opposed to being displaced by the polymer (a polymer-coated AuNP has a diameter of (12.2 ± 0.5) nm). After overnight stirring at room temperature, excess protein and polymer was removed by iterative centrifugation and subsequent resuspension of the AuNPs. The AuNP cores were then removed by oxidative dissolution in the presence of KCN and O_2. The resulting solution contains structures that have an average hydrodynamic diameter of (21.9 ± 1.3) nm, which is consistent with the conclusion that the protein–nanopod conjugates had formed. The slight size expansion post-dissolution of the gold is also consistent with our previous findings involving DNA-modified structures.[6] Throughout the dissolution process, the solution remained red in color, indicating that a protective layer is formed around the AuNPs. Control samples lacking the polymer turn purple instantly upon addition of KCN (1 μM final concentration), as a result of NP destabilization and aggregation.[12]

To prove that the proteins were incorporated into the polymer shell, a colorimetric assay was performed that requires the function of both proteins. The SA–HRP nanopods and controls were incubated over a biotin-functionalized surface, followed by washing under sonication using 1x phosphate-buffered saline with 0.05 % Tween-20. The surface was then treated with a TMB/H_2O_2 developing solution. Indeed, SA–HRP nanopods gave a positive readout (blue color), indicating the successful formation of the desired structures (Figure 2B). Conversely, control samples lacking either SA or polymer **1** did not show the blue color, ruling out the possibility of nonspecific HRP binding to the surface. Another series of controls involve particles containing the AuNP cores. Again, a lack of SA in the polymer particle leads to a colorless solution. However, in the absence of polymer **1**, the solution still turns blue since the AuNP can act as a support for the proteins. These results are also consistent with the conclusion that the SA- and HRP-cross-linked nanopods have successfully formed. In addition, the synthesis allows one to conveniently control the size of the conjugate. For example, we synthesized relatively monodisperse (44.6 ± 3.3) nm SA–HRP nanopods from (28.2 ± 0.5) nm AuNP templates (see the Supporting Information). Tang and co-workers have recently developed a novel protein nanocapsule by interfacial polymerization, which forms a polymer "cocoon" around the protein that serves to protect it from proteolysis.[13] The method described herein yields nanopod structures that are distinct from such protein-encapsulated entities; indeed, the proteins in the nanopods are incorporated in their walls and still capable of interacting with antigens.

With these results demonstrating that the entrapped proteins remain active, we designed and synthesized prototypical IPs. We chose the human epidermal growth factor receptor 2 (HER2), a member of the ErbB protein family, as the target antigen. This cell membrane surface-bound receptor tyrosine kinase is involved in signal transduction pathways leading to cell growth and differentiation.[14] Overexpression occurs in approximately 30 % of breast cancers,[15] as well as other cancers such as ovarian cancer, stomach cancer, and biologically aggressive forms of uterine cancer. Consequently, HER2 is of significant diagnostic and therapeutic importance.

To enable direct, optical observation of the polymer component of the IPs, polymer **1** was tagged with fluorescein 488-azide by using Cu^I-catalyzed click chemistry at a 1:1 polymer/dye molar stoichiometry. The formation of anti-HER2 IPs was monitored and confirmed by DLS (Figure S1 in the Supporting Information). After polymer and antibody adsorption, cross-linking, and subsequent core removal, the resulting IPs are (22.8 ± 2.2) nm (10 nm template) and (41.0 ± 2.9) nm (30 nm template). TEM images of the anti-HER2 IPs confirms the removal of the gold cores and show a spherical morphology (Figure 3A and S2 in the Supporting Information). Using fluorophore-labeled Abs and polymer, we determined the average number of Abs and polymer chains per particle type. For the 10 nm AuNP-templated IPs, each particle contains on average 3 Abs and 18 polymer chains, while the larger 30 nm AuNP-templated IPs have 22 Abs and 104 polymer chains per particle.

To determine if the Abs were stably incorporated within the walls of the IPs, we subjected the IPs to native

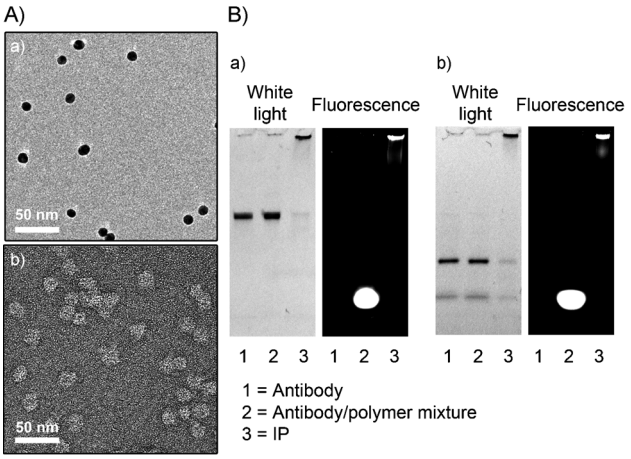

Figure 3. A) TEM images of a) ca. 10 nm AuNPs and b) IPs synthesized from ca. 10 nm AuNPs (negatively stained using uranyl acetate). B) SDS-PAGE of IPs and controls under a) native and b) denaturing conditions. The antibody and the IP can be observed by white light while the polymer component alone cannot be observed. By fluorescence in this experiment, the polymer and IP can be observed but not the antibody, which was not labeled.

polyacrylamide gel electrophoresis (PAGE) and sodium dodecyl sulfate PAGE (SDS-PAGE), using free Abs and Ab/polymer mixtures as controls. The Abs and IPs can be visualized by Coomassie blue staining and fluorophore excitation, respectively. If van der Waals interactions are responsible for maintaining the structural integrity of the IPs, high surfactant concentrations (10% w/v SDS) are expected to free the Abs from the IPs. Without heat-denaturation, free Ab displays a single band (Figure 3B a). The control mixture containing free Abs and polymer shows two respective bands, one for the Abs under white light and one for the polymer under fluorescent light, under identical conditions, indicating that they have little interaction in solution, or that their interaction can be eliminated by SDS. Importantly, the IPs show only one band of much higher molecular weight, consistent with covalent cross-linking of the Abs within the walls of the nanopod. A small amount (<6% by band density analysis) of free Abs is also observed. To test if the IPs remain a single entity under even harsher conditions, we attempted to denature the samples at 95°C for 5 min, where the light chain and heavy chain of the Ab are known to separate in the presence of SDS.[16] Remarkably, the majority of the denatured Ab chains (ca. 78%) remain attached to the polymer nanopod, while a small amount dissociate, as shown by faint bands in the gel electrophoresis analysis (Figure 3B b, left panel lane 3). These results are consistent with our hypothesis that the proteins are involved in covalent cross-linking within the polymer nanopods, likely through the hydroamination, hydroalkyoxylation, or hydrothiolation of the polymer alkynes by the respective nucleophilic side residues of the antibody (lysine, serine, or cysteine).[2a,17]

Having demonstrated that the IPs are stable in solution, we investigated if the IPs are capable of binding to target molecules. We designed and performed a competitive binding assay to quantitatively measure the relative binding affinity of the IPs. In this assay, free, biotin-functionalized Abs and IPs were mixed at various ratios, and allowed to compete for surface-immobilized HER2. Thereafter, a SA–HRP conjugate was used to detect the biotin-Ab. Apparent dissociation constants ($(K_d)_{app}$) can be derived from the binding isotherms (Figure S3 in the Supporting Information). We found that the $(K_d)_{app}$ value for IPs is 6.7 times that of the biotin-Ab, likely because of the higher steric hindrance on the surface of the IPs. In contrast, bovine serum albumin (BSA) and anti-His IPs (off-target IPs) show ca. 4000-fold higher $(K_d)_{app}$ values, as a result of nonspecific binding. Therefore, the IPs can still be considered as good binders.

To test cancer cells targeting in vitro, we incubated MCF-7 cells expressing HER2 (human breast adenocarcinoma cell line) for 30 min at 4°C with IPs at a concentration of 10 nM, followed by staining with a Northern Light 637 (NL637) labeled secondary antibody. A free Ab/polymer mixture (1:6 molar ratio, identical concentration as IP) was used as a negative control. We tracked the Abs and the fluorescein-labeled polymer nanopods independently by confocal fluorescence microscopy. Strikingly, while both control samples and the IPs exhibit fluorescence from the secondary antibody, only the IPs show significant fluorescence emitting from the

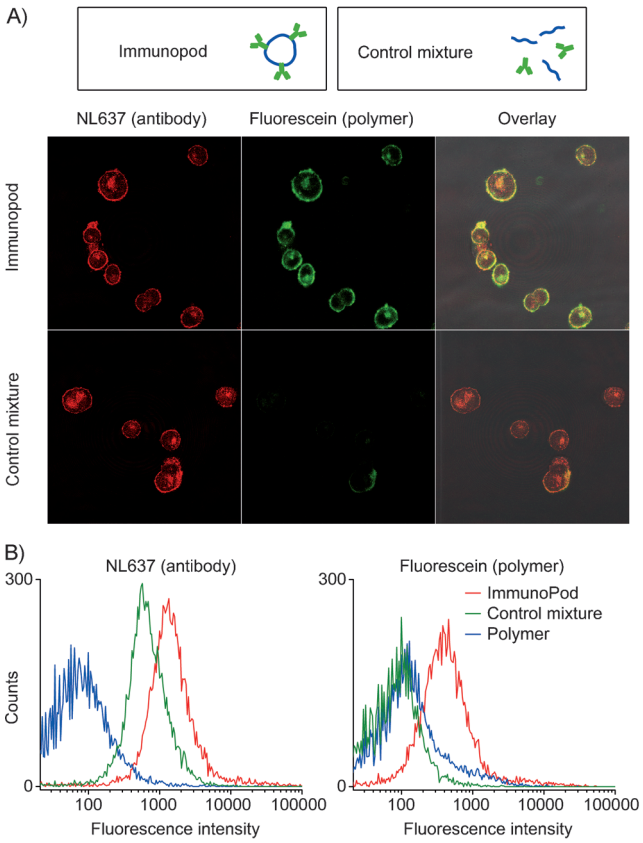

Figure 4. A) Confocal microscopy images of MCF-7 cells treated with 10 nM anti-HER2 IPs (top row) and a control mixture containing equivalent concentrations (10 nM) of free antibody and polymer (bottom row). While antibody binding is observed for both IPs and the control mixture, polymer association with cells is only significant when the IPs are used. B) Flow cytometry analysis of IP binding. Left: antibody (NL637) channel. Right: polymer nanopod (fluorescein) channel.

polymer nanopods; the fluorescence of the polymer also colocalizes with the antibody fluorescence (Figure 4A). Minimal polymer fluorescence was observed for the control sample. In contrast, anti-His IPs gave no fluorescent signals in both channels.

These observations are further confirmed by flow cytometry. Cells treated with IPs show 18.5 times more Ab fluorescence and 3.8 times more polymer fluorescence than free-polymer-treated cells, while cells treated with free antibody/polymer control mixture only exhibit Ab fluorescence (Figure 4B). An interesting observation is that the IP-treated cells show 2.8 times more Ab fluorescence than those treated with the control mixture, which contained free Abs. This observation is likely because the IPs contain multiple copies of Abs. Because the total number of HER2 proteins presented on the surface of the cell is limited, binding to the IPs results in greater fluorescence since more Abs are immobilized as compared to the free Ab case (there are three Abs per IP).

In conclusion, we have developed a convenient, one-pot method to create IPs, polymer nanopods cross-linked with native Abs, which remain biologically active. These structures can be made with tight control over their size and dispersity by virtue of the AuNP templates. Importantly, this strategy, in principle, can be expanded to other alkyne-bearing polymers, proteins, or other biomolecules to create a very diverse and potentially useful new class of bioconjugates.

Received: September 6, 2011
Revised: November 15, 2011
Published online: December 15, 2011

Keywords: antibodies · gold · HER2 · polymers · nanoparticles

[1] K. Zhang, J. I. Cutler, J. A. Zhang, D. Zheng, E. Auyeung, C. A. Mirkin, *J. Am. Chem. Soc.* **2010**, *132*, 15151 – 15153.
[2] a) Z. Li, C. Brouwer, C. He, *Chem. Rev.* **2008**, *108*, 3239 – 3265; b) A. S. K. Hashmi, *Chem. Rev.* **2007**, *107*, 3180 – 3211; c) S. Hotha, S. Kashyap, *J. Am. Chem. Soc.* **2006**, *128*, 17153 – 17153.
[3] a) X. Xu, W. L. Daniel, W. Wei, C. A. Mirkin, *Small* **2010**, *6*, 623 – 626; b) Y. Song, X. Xu, K. W. MacRenaris, X.-Q. Zhang, C. A. Mirkin, T. J. Meade, *Angew. Chem.* **2009**, *121*, 9307 – 9311; *Angew. Chem. Int. Ed.* **2009**, *48*, 9143 – 9147; c) D. A. Giljohann, D. S. Seferos, W. L. Daniel, M. D. Massich, P. C. Patel, C. A. Mirkin, *Angew. Chem.* **2010**, *122*, 3352 – 3366; *Angew. Chem. Int. Ed.* **2010**, *49*, 3280 – 3294; d) D. A. Giljohann, C. A. Mirkin, *Nature* **2009**, *462*, 461 – 464; e) D. Kim, W. L. Daniel, C. A. Mirkin, *Anal. Chem.* **2009**, *81*, 9183 – 9187; f) N. L. Rosi, C. A. Mirkin, *Chem. Rev.* **2005**, *105*, 1547 – 1562; g) O. R. Miranda, X. Li, L. Garcia-Gonzalez, Z.-J. Zhu, B. Yan, U. H. F. Bunz, V. M. Rotello, *J. Am. Chem. Soc.* **2011**, *133*, 9650 – 9653.
[4] a) S. Dhar, W. L. Daniel, D. A. Giljohann, C. A. Mirkin, S. J. Lippard, *J. Am. Chem. Soc.* **2009**, *131*, 14652 – 14653; b) M. E. Napier, J. M. DeSimone, *Polym. Rev.* **2007**, *47*, 321 – 327; c) O. C. Farokhzad, R. Langer, *ACS Nano* **2009**, *3*, 16 – 20.
[5] a) H. M. Xiong, D. van der Lelie, O. Gang, *J. Am. Chem. Soc.* **2008**, *130*, 2442 – 2443; b) R. J. Macfarlane, M. R. Jones, A. J. Senesi, K. L. Young, B. Lee, J. Wu, C. A. Mirkin, *Angew. Chem.* **2010**, *122*, 4693 – 4696; *Angew. Chem. Int. Ed.* **2010**, *49*, 4589 – 4592; c) M. R. Jones, R. J. Macfarlane, B. Lee, J. Zhang, K. L. Young, A. J. Senesi, C. A. Mirkin, *Nat. Mater.* **2010**, *9*, 913 – 917; d) C. A. Mirkin, R. L. Letsinger, R. C. Mucic, J. J. Storhoff, *Nature* **1996**, *382*, 607 – 609; e) J. N. Hunt, K. E. Feldman, N. A. Lynd, J. Deek, L. M. Campos, J. M. Spruell, B. M. Hernandez, E. J. Kramer, C. J. Hawker, *Adv. Mater.* **2011**, *23*, 2327 – 2331; f) K. Y. van Berkel, C. J. Hawker, *J. Polym. Sci. Part A* **2010**, *48*, 1594 – 1606.
[6] J. I. Cutler, K. Zhang, D. Zheng, E. Auyeung, A. E. Prigodich, C. A. Mirkin, *J. Am. Chem. Soc.* **2011**, *133*, 9254 – 9257.
[7] a) M. Shi, J. Lu, M. S. Shoichet, *J. Mater. Chem.* **2009**, *19*, 5485 – 5498; b) G. T. Hermanson, *Bioconjugation Techniques*, 2nd ed., Elsevier, Rockford, IL, **2008**.
[8] I.-H. Cho, E.-H. Paek, H. Lee, J. Y. Kang, T. S. Kim, S.-H. Paek, *Anal. Biochem.* **2007**, *365*, 14 – 23.
[9] M. M. J. Kamphuis, A. P. R. Johnston, G. K. Such, H. H. Dam, R. A. Evans, A. M. Scott, E. C. Nice, J. K. Heath, F. Caruso, *J. Am. Chem. Soc.* **2010**, *132*, 15881 – 15883.
[10] S. Egli, M. G. Nussbaumer, V. Balasubramanian, M. Chami, N. Bruns, C. Palivan, W. Meier, *J. Am. Chem. Soc.* **2011**, *133*, 4476 – 4483.
[11] a) J. Turkevich, P. C. Stevenson, J. Hillier, *Discuss. Faraday Soc.* **1951**, *11*, 55 – 75; b) G. Frens, *Colloid Polym. Sci.* **1972**, *250*, 736 – 741.
[12] M. C. Daniel, D. Astruc, *Chem. Rev.* **2004**, *104*, 293 – 346.
[13] a) Z. Gu, M. Yan, B. Hu, K.-I. Joo, A. Biswas, Y. Huang, Y. Lu, P. Wang, Y. Tang, *Nano Lett.* **2009**, *9*, 4533 – 4538; b) M. Yan, J. Du, Z. Gu, M. Liang, Y. Hu, W. Zhang, S. Priceman, L. Wu, Z. H. Zhou, Z. Liu, T. Segura, Y. Tang, Y. Lu, *Nat. Nanotechnol.* **2010**, *5*, 48 – 53.
[14] M. Pegram, D. Slamon, *Semin. Oncol.* **2000**, *27*, 13 – 19.
[15] a) D. J. Slamon, G. M. Clark, S. G. Wong, W. J. Levin, A. Ullrich, W. L. Mcguire, *Science* **1987**, *235*, 177 – 182; b) J. J. Isola, K. Holli, H. Oksa, Y. Teramoto, O. P. Kallioniemi, *Cancer* **1994**, *73*, 652 – 658.
[16] A. L. Shapiro, E. Viñuela, J. V. J. Maizel, *Biochem. Biophys. Res. Commun.* **1967**, *28*, 815 – 820.
[17] A. Corma, C. González-Arellano, M. Iglesias, F. Sánchez, *Appl. Catal. A* **2010**, *375*, 49 – 54.

